Effects of Hemicellulose on Recycling Performance of Paper Based on Sisal Fibers

Shaoliu Qin
Guangxi University
Yian Chen (chenyian@scut.edu.cn)
South China University of Technology
Shenming Tao
South China University of Technology
Cunzhi Zhang
South China University of Technology
Xingzhen Qin
Guangxi University
Pan Chen
Beijing Institute of Technology
Haisong Qi
South China University of Technology

Research Article

Keywords: Recycling, Holocellulose, Hornification, Mechanical properties

Posted Date: July 6th, 2021

DOI: https://doi.org/10.21203/rs.3.rs-610216/v1

Abstract

The pulp and paper industry growingly paid attention to the recycling and maintenance of waste paper products. Each paper-making cycle would lead to a sharp drop in the mechanical properties of the cellulosic paper, which was related to the hornification effect. Here, the recycling performance of the holocellulose paper was studied, compared with that of the cellulosic paper. Holocellulose fibers from sisal were fabricated by a gentle delignification method, and the well-preserved cellulose and hemicellulose components hindered the cocrystallization and aggregation of cellulose fibril. Holocellulose paper exhibited much more favorable recycling properties, compared with cellulosic paper. After 5 runs of recycling, holocellulose paper still shown an ultimate strength as high as 25 MPa (reduced from 35 MPa), a decrease of 27.1 %. However, cellulosic paper experienced a substantial loss in ultimate strength from 35 MPa to 9 MPa, a decrease of about 74 %. This can be attributed to the core-shell structure from cellulose and hemicellulose to weaken the hornification effect.

Introduction

The disposal of waste paper had always attracted much attention in the paper industry(Luo et al., 2003). Simply discarding it for natural degradation or incineration would cause a waste of biomass resources. Meanwhile, it was likely to cause environmental pollution and unexpected natural accidents, such as soil pollution and fire disaster(Ouadi et al., 2019). Therefore, an environmentally friendly strategy to utilize waste paper and produce new recycled paper was of importance(Jeong et al., 2018). It could reduce the burden of environmental pollution and improve economic benefits(Lin et al., 2020). For instance, the recycling rate of waste paper in China had reached a high level (70%) in 2017. Meanwhile, the recycling of waste paper was an effective way to reduce carbon emissions in China's paper industry(Shang et al., 2021). However, the mechanical strength of the paper would drop to a frustrating level during the recycling process, compared with the original paper fiber(Janda, 1995). Fiber qualities would undergo an irreversible decline when recycled paper fiber was exposed to cycles of wetting and drying. In detail, the morphology of the cellulosic fiber had changed during the recycling process(Mendes et al., 2019), fibers trended to aggregate and formed a more compact structure(Ponni et al., 2012). The amorphous area of the fiber was more easily degraded, and relatively, the crystallinity became larger, which made it more difficult to disperse into a single fiber. The term "hornification" aptly described this phenomenon, the degree to which fibers were irreversibly combined when they were dried or rewet(Cid et al., 2020; Mendes et al., 2019; Yang and Berglund, 2020). High-strength beating was intended to disperse the fibers as much as possible(Chen et al., 2012). It was the most commonly used method to overcome the effects of hornification(Suchy et al., 2010). Furthermore, the addition of fiber binder or fresh fiber can also improve the mechanical properties of recycled paper(Santmarti et al., 2020; Tavast et al., 2014; Yang and Pelton, 2017). However, the recycled paper was not able to fully recovered to the performance of the original paper.

Hemicellulose, as a substance without crystalline regions, was tightly wrapped on the surface of cellulose(Terrett and Dupree, 2019). It could be intimately integrated into cellulose fibers and hinder the

hornification of cellulose paper during recycling processes(Déléris and Wallecan, 2017; Köhnke et al., 2010; Lavoine et al., 2012). Meanwhile, holocellulose fibers with native hemicellulose well-preserved cellulose could be obtained through delignification of wood or other plants. The delignification method was consisted of the peracetic acid method(Palamae et al., 2014; Zhao et al., 2011), chlorine dioxide method(Acharjee et al., 2017; Barroca et al., 2001), chlorine bleaching method(Axegård, 2019), and sodium chlorite method(Jin et al., 2019). The sodium chlorite method was called the Wise method that the purpose of continuous delignification was achieved by circulating added sodium chlorite and glacial acetic acid(Hubbell and Ragauskas, 2010). The sodium chlorite method was one of the most common methods to selectively remove lignin in industry scale. The main product in this reaction was chlorine dioxide, and chloride and chlorate, as the secondary products(Siqueira et al., 2013). It took into account a high selectivity and low environmental impact. Therefore, the sodium chlorite method was still a commonly used method in laboratories.

These hemicellulose-rich holocellulose fibers would be suitable for the investigation of the recycling potential. Moreover, it was interesting to compare the recycling performance between holocellulose paper and cellulose paper from the same raw material. In this study, holocellulose paper was prepared via the sodium chlorite method, followed by the defibering and paper-making process. As a comparison, an extra alkali treatment was carried out to remove hemicellulose from holocellulose fibers, and thereby achieve cellulose paper. Then, the recycling performance of two kinds of paper was investigated comprehensively.

Experiment

Material

Native sisal was brought from a local market. Acetone (99%), absolute ethanol (99.7%), sodium chlorite (80%), glacial acetic acid (99.5%) and other chemical reagents were purchased from Shanghai Macklin Biochemical Co., Ltd., China and implemented without further purification.

Preparation of sisal holocellulose and cellulosic fiber

First, sisal leaves were cut into a rectangle shape with 1 cm *1.5 cm size, then washed and dried. 50 g of dried sisal leaves were soaked in 500 mL acetone overnight to dewax, and then washed repeatedly with deionized water and ethanol until the acetone was completely removed. Then, sisal leaves (10 g) after dewax were added into the aqueous solution (350 mL) with sodium chlorite (3.75 g) and glacial acetic acid (3 mL) for 1.0 h at 75 °C. The same amount of sodium chlorite and glacial acetic acid was added every hour for 4 times. Finally, the resultant product was repeatedly washed by running water to remove the residual chemicals. In order to beat the product into fine holocellulose fiber, the product was added into a Vitamix Blenders (20000 rpm, TNC5200, USA) for 3 minutes. Cellulosic fibers were obtained by adding holocellulose fibers into the NaOH aqueous solution at 90 °C for 2.0 h.

Paper making and recycling process

A Rapid Köthen (RK3AKWT, Austria) was carried out for paper making. The paper with a targeting weight per surface area at 165 g/m^2 was dried at 90 °C and 0.1 MPa for 10 min. During the recycling process, the holocellulose paper was torn into small pieces and soaked in water. Then, it was dispersed into a slurry used a fiber fluffer at 5000 revolutions and made into paper again. A total of 10 times were recycled, and the obtained papers with different recycling times was named holocellulose-0~10. The cellulose paper was recycled 5 times in the same way and named cellulose-0~5.

Characterizations

The acid-insoluble lignin content of sisal holocellulose was determined through the GB-T2677.8-1994 standard. The obtained monosaccharide solution was adjusted to a concentration of 1000 ppm. The content of cellulose and hemicellulose was measured by a high pressure liquid chromatography (LC-100, USA) with a differential detector. A fiber analyzer (FS300, Finland) was performed to measure the length and width of the fiber. A universal material testing machine (INSTRON 5565, USA) was carried out to test the mechanical tensile properties of the holocellulose paper, and each paper was tested three times. Fourier transform infrared spectrometer-infrared (FT-IR) microscope (Nicolet IS50-Nicolet Continuum, USA) was recorded to test the groups of recycled paper and the self-reinforcing paper. A multi-position automatic sampling X-ray diffractometer (XRD, X'pert Powder, PANalytical) was used to determine the crystallinity of the holocellulose paper with a conventional wide-angle from 5 ° to 60 ° at a scanning speed of 12 °/min. The crystallinity index (*CrI*) was calculated by the peak strength method as follows: (Segal et al., 1959)

$$CrI = \frac{I_{200} - I_{am}}{I_{200}} \qquad (1)$$

Note: I_{200} was the diffracted intensity of crystallographic area at $2\theta \approx 22.5°$. I_{am} was the diffracted intensity of the amorphous region at $2\theta \approx 18.8$ °.

The holocellulose paper with a size of 6 cm *10 cm was carried out by a 0-spacing tensile strength tester (Z-span 2400, Canada) to test the 0-span tensile strength.

The water retention values (WRV) of recycled paper were calculated by the ISO 23714:2014 standard. In detail, about 1 g of pulp was centrifuged at 3000 g for 30 min to remove water and weighed. Then, the resultant pulp was dried at 105 °C for 24 hours and weighed again. The following was the calculation formula for WRV:

$$WRV(\%) = \frac{m_{wet} - m_{dry}}{m_{dry}} \times 100\% \qquad (2)$$

Note: m_{wet} was the mass of the pulp before drying, and m_{dry} was the dry weight of the pulp.

The following was the formula for calculating the degree of hornification (DOH)：

$$DOH(\%) = \frac{WRV_0 - WRV_n}{WRV_0} \times 100\% \qquad (3)$$

Note: WRV_0 was the water retention value of holocellulose-0 and WRV_n was the water retention value of holocellulose-n.

The surface morphology and fiber morphology of the tensile fracture surface was observed by a field emission scanning electron microscope (SEM) (EVO 18, Germany).

Results And Discussion

Figure 1 described the entire paper making and recycling process. The raw material extraction process was divided into two steps. Firstly, the holocellulose was extracted by gentle delignification, and then the hemicellulose in the holocellulose was destroyed by alkali treatment. Holocellulose fibers and cellulose fibers were obtained by the above two steps. During the typical paper making process, the holocellulose/cellulose was defibered and then filtered through the vacuum to obtain wet cake. The Kaiser system can simply and quickly remove the moisture to obtain a dense paper. During the recycling process, the paper was torn into small pieces and then placed in the fiber decomposer. The strong force would redistribute the small pieces of paper into a free fiber state so that the paper could be made again. In each cycle process, changes in fiber morphology and recycled paper properties would occur. It was of importance and meaningful to explore the evolution of the morphology and recycling performance of holocellulose paper during the recycling process.

With the same targeting weight per surface area at 165 g/m^2, holocellulose paper with a smooth surface (Fig. 1B) possessed higher thickness (240 μm) and lower density (0.69 g/ cm^3), compared to that of cellulosic paper (230 μm, 0.76 g/ cm^3) (Table 1). Native hemicellulose would expand the interfibrillar space between cellulose fibers during the paper making process, resulting in lower density and higher porosity of holocellulose paper (Yang and Berglund, 2020). As SEM images shown in Fig. 1B, Fibers in holocellulose paper appear similar in structure compared with cellulosic paper in size and distribution (Fig. 1B and 1C).

As shown in Fig. 2A and Table 1, the ultimate strength of holocellulose was close to that of cellulosic paper, supported by the SEM results in Fig. 1B and 1C. Moreover, compared with cellulosic paper, holocellulose paper exhibited a lack of strain-softening, due to the favorable interfiber bonding in holocellulose paper with native hemicellulose. Upon recycling, the mechanical properties of cellulosic paper decreased significantly, which was attributed to the hornification effect of cellulose fibers. In contrast, holocellulose paper showed no apparent changes in the mechanical performance (Fig. 2B). For example, as shown in Fig. 2C, the ultimate tensile strength (σ_u) of holocellulose paper was higher than that of cellulosic paper during the recycling process. After 5 runs of recycling, holocellulose paper still

shown an ultimate strength as high as 25 MPa (a decrease of 27.1%), while cellulosic paper experienced a substantial loss in ultimate strength from 35 MPa to 9 MPa, a decrease of about 74%. Meanwhile, the strain to failure of cellulose paper showed rapidly dropped after 2 runs of recycling from 4.28 to 2.50, a decrease of 41.6% (Fig. 2D), while this phenomenon did not appear in the recycling process of holocellulose paper. Similarly, the Young's modulus of elasticity (E) calculated from Fig. 2A and Fig. 2B exhibited favorable performance of holocellulose paper, as shown in Fig. 2E. After 8 runs of recycling, holocellulose paper presented a Young's modulus of elasticity as high as 1.1 GPa (a decrease of 17%). Moreover, after 5 runs of recycling, the 0-span tensile strength of holocellulose paper showed not changed (115 N/cm), while the cellulosic paper displayed an obvious decrease (Fig. 2F and Table 1). Consequently, holocellulose paper showed favorable recycling performance related to the mechanical properties compared with cellulosic paper.

The content of cellulose and hemicellulose was measured by high pressure liquid chromatography. Although holocellulose fiber was obtained by the delignification process, as showed in Fig. 3A and Table S1, holocellulose fiber was consisted of cellulose (~ 77%), hemicellulose (~ 10%), and lignin (~ 7.5%). Hemicellulose was destroyed by treated with an alkali solution to obtain cellulose(Carvalho et al., 2019; Zhang et al., 2020). Upon recycling process, the content of hemicellulose slightly decreased, indicating a small amount loss of hemicellulose during the paper making procedure. Thus, this result strongly supported that the presence of hemicellulose was conducive to the recycling performance of holocellulose paper compared with cellulosic paper.

Table 1

Mechanical properties of holocellulose and cellulose paper with different cycles[a]

Type	Thickness (μm)	Density (g/cm^3)	Porosity (%)	0-span tensile strength (N/cm)	E^b (MPa)	$\sigma_u{}^c$ (MPa)	γ^d (%)
Holocellulose-0	240 (10)	0.69 (0.02)	54 (0.01)	115 (0)	1368 (200)	35.20 (1.09)	4.28 (0.33)
Holocellulose-1	250 (10)	0.66 (0.01)	56 (0.01)	115 (0)	1335 (100)	33.65 (2.26)	4.39 (0.46)
Holocellulose-2	250 (10)	0.66 (0.01)	56 (0.01)	115 (0)	1266 (100)	30.17 (0.98)	3.94 (0.31)
Holocellulose-3	260 (10)	0.65 (0.02)	57 (0.01)	115 (0)	1131 (100)	29.32 (0.35)	3.78 (0.35)
Holocellulose-4	240 (10)	0.68 (0.01)	55 (0.01)	115 (0)	1251 (100)	27.13 (0.98)	3.51 (0.23)
Holocellulose-5	270 (10)	0.63 (0.01)	58 (0.01)	115 (0)	1159 (100)	24.58 (0.74)	3.45 (0.18)
Holocellulose-6	280 (10)	0.60 (0.04)	60 (0.03)		1152 (100)	22.56 (1.07)	3.17 (0.06)
Holocellulose-7	280 (10)	0.61 (0.01)	59 (0.01)		1137 (60)	20.96 (0.88)	3.23 (0.25)
Holocellulose-8	280 (10)	0.61 (0.05)	59 (0.04)		1131 (60)	19.07 (1.62)	2.94 (0.33)
Holocellulose-9	280 (10)	0.61 (0.02)	59 (0.02)		1080 (90)	17.50 (0.07)	2.78 (0.20)
Holocellulose-10	280 (10)	0.60 (0.02)	60 (0.01)		948 (120)	14.94 (0.53)	2.55 (0.15)
Cellulose-0	230 (10)	0.76 (0.04)	49 (0.02)	115 (0)	1408 (300)	34.48 (5.14)	4.72 (0.88)

[a] Standard deviations reported in parentheses. [b] Young's modulus of elasticity. [c] Ultimate tensile strength. [d] Strain to failure.

Type	Thickness (μm)	Density (g/cm^3)	Porosity (%)	0-span tensile strength (N/cm)	E^b (MPa)	$\sigma_u{}^c$ (MPa)	γ^d (%)
Cellulose-1	240 (10)	0.69 (0.04)	54 (0.03)	113 (2)	1397 (400)	24.53 (2.26)	4.28 (0.56)
Cellulose-2	270 (10)	0.61 (0.03)	59 (0.02)		991 (200)	14.92 (1.24)	2.50 (0.24)
Cellulose-3	270 (10)	0.62 (0.06)	59 (0.04)	110 (5)	872 (300)	12.27 (1.37)	2.55 (0.51)
Cellulose-4	290 (10)	0.58 (0.01)	61 (0.01)		902 (200)	11.35 (1.97)	2.56 (0.67)
Cellulose-5	270 (10)	0.63 (0.04)	58 (0.03)	110 (6)	824 (230)	8.85 (1.80)	1.67 (0.67)

[a] Standard deviations reported in parentheses. [b] Young's modulus of elasticity. [c] Ultimate tensile strength. [d] Strain to failure.

To further clarify how the native hemicellulose affects the recycling performance, the FT-IR spectra of holocellulose and cellulosic paper with different runs of recycling were studied in Figure 3B. The strong absorption at 1030 cm^{-1} and 3418 cm^{-1} were due to the C-O-C stretching vibration and the O-H stretching vibration, respectively(Benítez-Guerrero et al., 2016). There was a clear difference between holocellulose and cellulosic paper in terms of hydroxyl characteristic peaks. The hydroxyl characteristic peaks gradually increased with the recycling processes of cellulose paper. As expected, this suggested that cellulose fiber trended to aggregate and formed a more compact structure via irreversible hydrogen bonds during recycling processes, which was consistent with the decreased water retention value (WRV) and increased degree of hornification (DOH) displayed in Figure 3C and 3D. The reason for the degradation of recycling performance was attributed to the hornification effect between the fibers, which caused the fibers to be unable to reach the dispersion degree of the previous papermaking in the process of re-deflating. The change in water retention value was an important criterion that reflected the degree of hornification. The higher the water retention value, the fewer irreversible hydrogen bonds between fibers, and the better its dispersibility.

Moreover, during the recycling process, the crystallinity of cellulose calculated from XRD spectra (Figure S1) increased significantly after different runs of recycling. In contrast, the small change of hydroxyl characteristic peak in Figure 3B and low DOH values shown in Table 2 jointly explained that hemicellulose in holocellulose paper could prevent the hornification effect. Combined with the above result, the slight changes of hemicellulose content (Figure 3A) during the recycling process could prevent the hornification effect and maintained the mechanical performance of holocellulose paper. Furthermore,

the SEM images could also explain the changes in the holocellulose and cellulose fiber structure at different cycle stages (Figure 4). All broken fibers in the image are from tensile tests. Interestingly, the tensile fracture surface of holocellulose-0 and holocllulose-5 fibers appeared flat, while cellulose-0 and cellulose-5 fibers appeared a larger deviation, indicating that the strong interfiber bonding was formed in holocellulose paper.

Table 2

Structural parameters of holocellulose fibers and cellulose fibers after different recycling times [a]

Type	Length[b] (mm)	Width[b] (μm)	WRV[c] (%)	DOH[d] (%)	Crystallinity (%)
Holocellulose-0	0.831	22.2	184 (5)		69.44
Holocellulose-1	0.833	21.0	181 (11)	1.6	
Holocellulose-2	0.892	21.3			
Holocellulose-3	0.862	21.3	177 (10)	3.8	72.46
Holocellulose-4	0.865	21.0			
Holocellulose-5	0.851	20.8	173 (9)	6.0	75.81
Cellulose-0	0.767	14.4	158 (5)		88.79
Cellulose-1	0.778	14.0	133 (4)	15.8	
Cellulose-2	0.791	13.7			
Cellulose-3	0.787	13.6	115 (11)	27.2	90.46
Cellulose-4	0.792	13.3			
Cellulose-5	0.799	13.1	114 (4)	27.8	90.42

[a]Standard deviations reported in parentheses. [b]Length and width are normally distributed data with the largest percentage of the measured value. [c]WRV, water retention value. [d]DOH, degree of hornification.

Conclusion

Through the gentle delignification method, the hemicellulose-rich holocellulose was prepared from sisal raw material. The recycling process of waste paper was simulated, compared with the performance changes of holocellulose paper and cellulose paper. After 5 times of recycling, the ultimate tensile strength of the holocellulose paper decreased by 27.1%, and after 10 times of recycling, the ultimate tensile strength decreased by 57.5%. The cellulose paper was recycled 5 times and it dropped by ~ 74%. It can be seen that the hemicellulose-rich holocellulose paper presented higher recycling performance than cellulose. From the fiber point of view, both holocellulose and cellulose, recycling processes would cause a trend of decreasing fiber width. The hemicellulose in the holocellulose assumes a sacrificial role,

reducing the damage suffered by the cellulose fiber during the recycling process. As a consequence, holocellulose had shown significant advantages in recycling processes, the fiber morphology would not change much during the recycling processes. The recyclability of fibers was greatly increased. Recycled paper was more competitive in terms of market demand.

Declarations

Acknowledgements

The authors are grateful for the financial support for this work by the National Natural Science Foundation of China (21774036), Guangdong Province Science Foundation (2017GC010429), Postdoctoral Science Foundation of China (2020TQ0107), and Science and Technology Program of Guangzhou (202002030329).

Ethics declarations

Conflict of interest

The authors declare that they have no conflicts of interest.

Ethical approval

This article does not contain any studies with human participants or animals performed by any of the authors. In this experiment, we did not collect any samples of humans and animals.

References

1. Acharjee, T.C., Jiang, Z., Haynes, R.D., and Lee, Y.Y. (2017). Evaluation of chlorine dioxide as a supplementary pretreatment reagent for lignocellulosic biomass. Bioresour Technol 244: 1049-1054.
2. Axegård, P. (2019). The effect of the transition from elemental chlorine bleaching to chlorine dioxide bleaching in the pulp industry on the formation of PCDD/Fs. Chemosphere 236: 124386.
3. Barroca, M.J.M.C., Marques, P.J.T.S., Seco, I.M., and Castro, J.A.A.M. (2001). Selectivity studies of oxygen and chlorine dioxide in the pre-delignification stages of a hardwood pulp bleaching plant. Ind Eng Chem Res 40: 5680-5685.
4. Benítez-Guerrero, M., Pérez-Maqueda, L.A., Artiaga, R., Sánchez-Jiménez, P.E., and Pascual-Cosp, J. (2016). Structural and chemical characteristics of sisal fiber and its components: effect of washing and grinding. J Nat Fibers 14: 26-39.
5. Carvalho, D.M.d., Moser, C., Lindström, M.E., and Sevastyanova, O. (2019). Impact of the chemical composition of cellulosic materials on the nanofibrillation process and nanopaper properties. Ind Crops Prod 127: 203-211.
6. Chen, Y., Wan, J., Zhang, X., Ma, Y., and Wang, Y. (2012). Effect of beating on recycled properties of unbleached eucalyptus cellulose fiber. Carbohydr Polym 87: 730-736.

7. Cid, S.C.G., Cardoso, D.C.T., Silva, F.d.A., and Krause, J.Q. (2020). Influence of hornification on the physical and flexural properties of Moso bamboo. Constr Build Mater 248: 118701.
8. Déléris, I., and Wallecan, J. (2017). Relationship between processing history and functionality recovery after rehydration of dried cellulose-based suspensions: A critical review. Adv Colloid Interface Sci 246: 1-12.
9. Hubbell, C.A., and Ragauskas, A.J. (2010). Effect of acid-chlorite delignification on cellulose degree of polymerization. Bioresour Technol 101: 7410-7415.
10. Janda, B.W. (1995). Advances in paper fiber recycling: Meeting the challenge. In Plastics, Rubber, and Paper Recycling (American Chemical Society), pp. 306-322.
11. Jeong, Y., Moon, K., Jeong, S., Koh, W.-G., and Lee, K. (2018). Converting waste papers to fluorescent carbon dots in the recycling process without loss of ionic liquids and bioimaging applications. ACS Sustain Chem Eng 6: 4510-4515.
12. Jin, K., Liu, X., Jiang, Z., Tian, G., Yang, S., Shang, L., and Ma, J. (2019). Delignification kinetics and selectivity in poplar cell wall with acidified sodium chlorite. Ind Crops Prod 136: 87-92.
13. Köhnke, T., Lund, K., Brelid, H., and Westman, G. (2010). Kraft pulp hornification: A closer look at the preventive effect gained by glucuronoxylan adsorption. Carbohydr Polym 81: 226-233.
14. Lavoine, N., Desloges, I., Dufresne, A., and Bras, J. (2012). Microfibrillated cellulose – Its barrier properties and applications in cellulosic materials: A review. Carbohydr Polym 90: 735-764.
15. Lin, L., Yang, J., Ni, S., Wang, X., Bian, H., and Dai, H. (2020). Resource utilization and ionization modification of waste starch from the recycling process of old corrugated cardboard paper. J Environ Manage 271: 111031.
16. Luo, Q., Deng, Y., Zhu, J., and Shin, W.-T. (2003). Foam control using a foaming agent spray: A novel concept for flotation deinking of waste paper. Ind Eng Chem Res 42: 3578-3583.
17. Mendes, S., Hugen, L.N., Dos Santos, R.D., Toledo Filho, R.D., and Ferreira, S.R. (2019). Influence of water amount and immersion time on the sisal fibers hornification process. J Nat Fibers, 1-10.
18. Ouadi, M., Fivga, A., Jahangiri, H., Saghir, M., and Hornung, A. (2019). A review of the valorization of paper industry wastes by thermochemical conversion. Ind Eng Chem Res 58: 15914-15929.
19. Palamae, S., Palachum, W., Chisti, Y., and Choorit, W. (2014). Retention of hemicellulose during delignification of oil palm empty fruit bunch (EFB) fiber with peracetic acid and alkaline peroxide. Biomass Bioenergy 66: 240-248.
20. Ponni, R., Vuorinen, T., and Kontturi, E. (2012). Proposed nano-scale coalescence of cellulose in chemical pulp fibers during technical treatments. Bioresources 7: 6077-6108.
21. Santmarti, A., Tammelin, T., and Lee, K.-Y. (2020). Prevention of interfibril hornification by replacing water in nanocellulose gel with low molecular weight liquid poly(ethylene glycol). Carbohydr Polym 250: 116870.
22. Segal, L., Creely, J.J., Martin, A.E., and Conrad, C.M. (1959). An empirical method for estimating the degree of crystallinity of native cellulose using the X-ray diffractometer. Text Res J 29: 786-794.

23. Shang, D., Diao, G., Liu, C., and Yu, L. (2021). The impact of waste paper recycling on the carbon emissions from China's paper industry. Environ Manage 67: 811-821.
24. Siqueira, G., Várnai, A., Ferraz, A., and Milagres, A.M.F. (2013). Enhancement of cellulose hydrolysis in sugarcane bagasse by the selective removal of lignin with sodium chlorite. Appl Energy 102: 399-402.
25. Suchy, M., Kontturi, E., and Vuorinen, T. (2010). Impact of drying on wood ultrastructure: Similarities in cell wall alteration between native wood and isolated wood-based fibers. Biomacromolecules 11: 2161-2168.
26. Tavast, D., Mansoor, Z.A., and Brännvall, E. (2014). Xylan from agro waste as a strength enhancing chemical in kraft pulping of softwood. Ind Eng Chem Res 53: 9738-9742.
27. Terrett, O.M., and Dupree, P. (2019). Covalent interactions between lignin and hemicelluloses in plant secondary cell walls. Curr Opin Biotechnol 56: 97-104.
28. Yang, D., and Pelton, R.H. (2017). Degradable microgel wet-strength adhesives: A route to enhanced paper recycling. ACS Sustain Chem Eng 5: 10544-10550.
29. Yang, X., and Berglund, L.A. (2020). Recycling without fiber degradation—Strong paper structures for 3D forming based on nanostructurally tailored wood holocellulose fibers. ACS Sustain Chem Eng 8: 1146-1154.
30. Yongjun, Yin.; Xueping, Song.; Chongxin, Li.; and Shuangxi, Nie. (2018). A method for integrated optimization of chlorine dioxide delignification of bagasse pulp. Bioresources 13: 1065-1074.
31. Zhang, C., Chen, G., Wang, X., Zhou, S., Yu, J., Feng, X., Li, L., Chen, P., and Qi, H. (2020). Eco-friendly bioinspired interface design for high-performance cellulose nanofibril/carbon nanotube nanocomposites. ACS Appl Mater Inter 12: 55527-55535.
32. Zhao, X., Wu, R., and Liu, D. (2011). Production of pulp, ethanol and lignin from sugarcane bagasse by alkali-peracetic acid delignification. Biomass Bioenergy 35: 2874-2882.

Figures

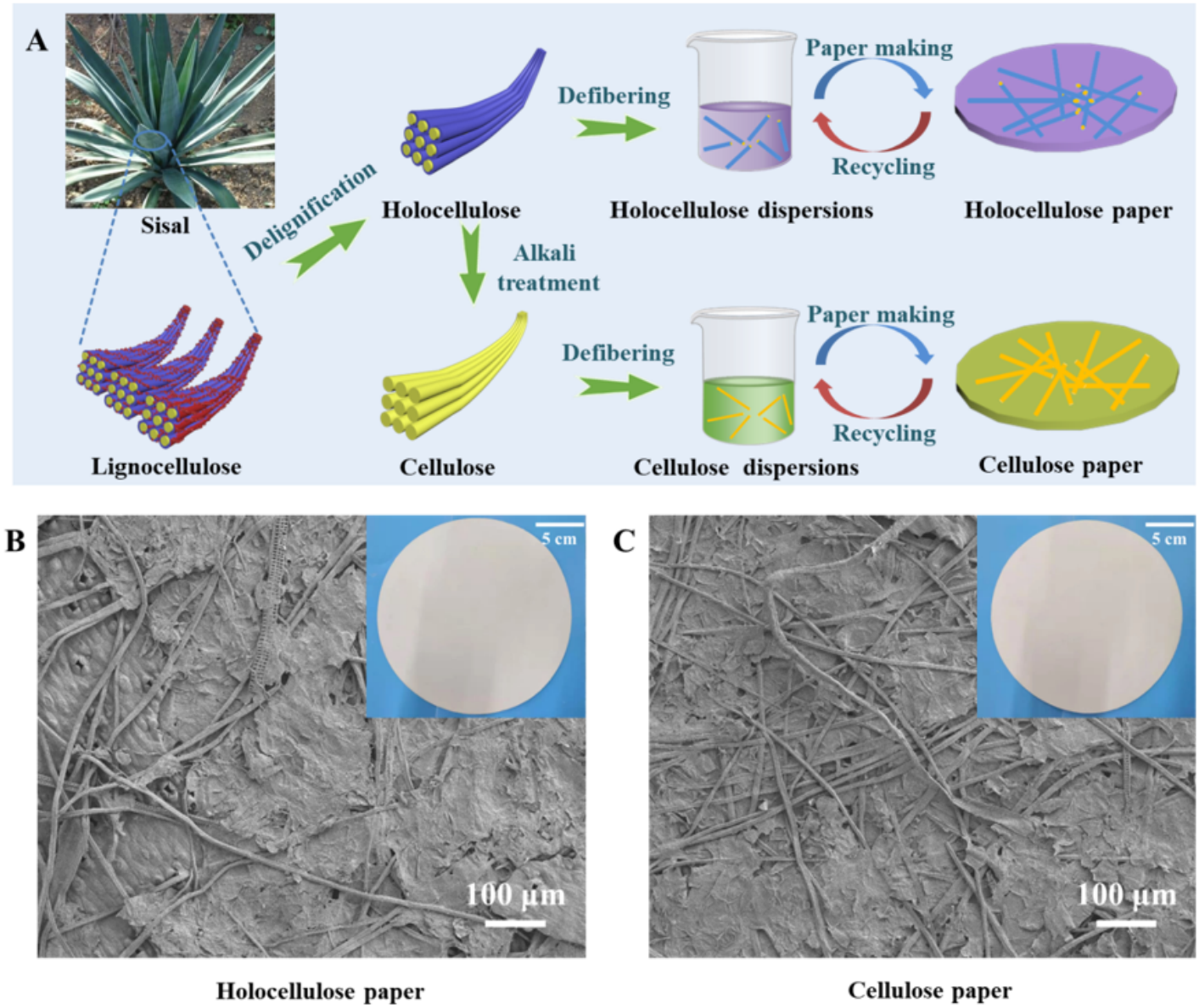

Figure 1

(A) Schematic diagram of raw material extraction from sisal to recycle paper. Optical view and SEM images of (B) holocellulose-0 paper, and (C) cellulose-0 paper.

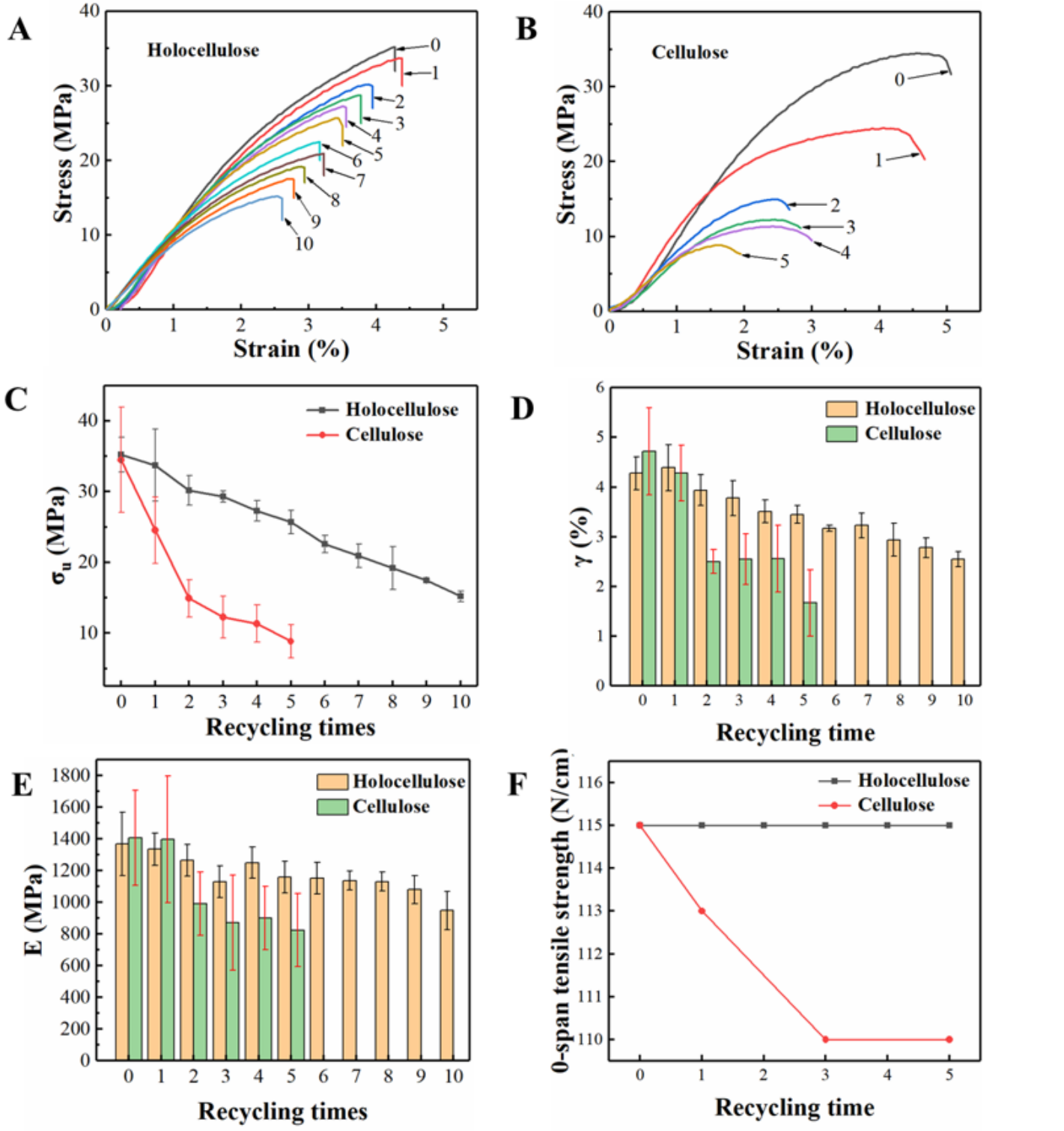

Figure 2

Diagram of mechanical performance: (A) stress – strain curve of holocellulose recycled 0-10 times and (B) cellulose recycled 0-5 times, (C) comparison of ultimate tensile strength, (D) strain to failure, (E) Young's modulus and (F) 0-span tensile strength of holocellulose and cellulose in different recycling time.

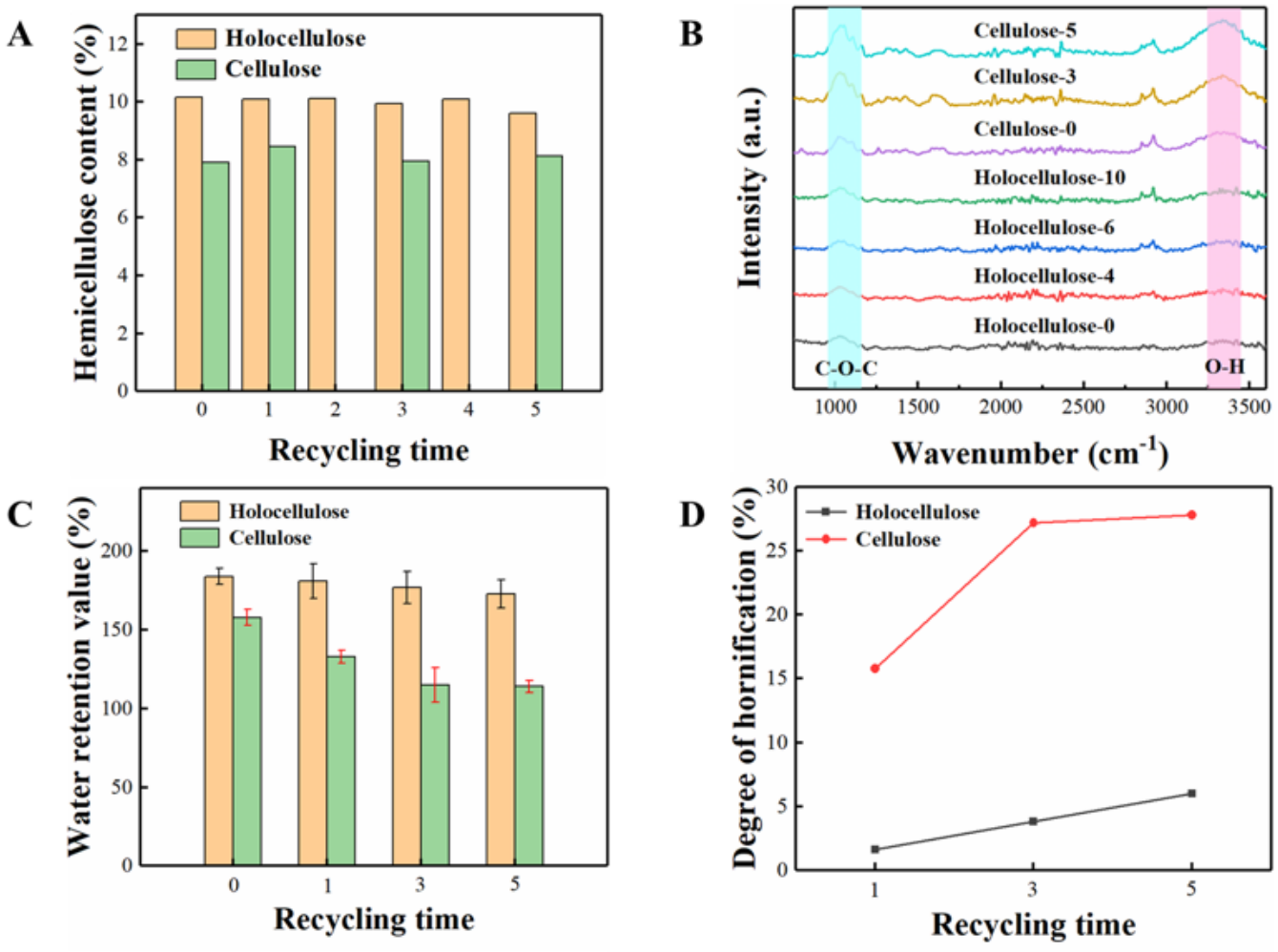

Figure 3

(A) hemicellulose content of holocellulose recycled 0-5 times and cellulose-0; (B) FT-IR spectra of holocellulose paper recycled times of: 0, 4, 6, 10 and cellulose paper recycled times of: 0, 3, 5 (C) water retention value of holocellulose and cellulose in recycling time of 0, 1, 3, 5; (D) degree of hornification of holocellulose and cellulose in recycling time of 1, 3, 5.

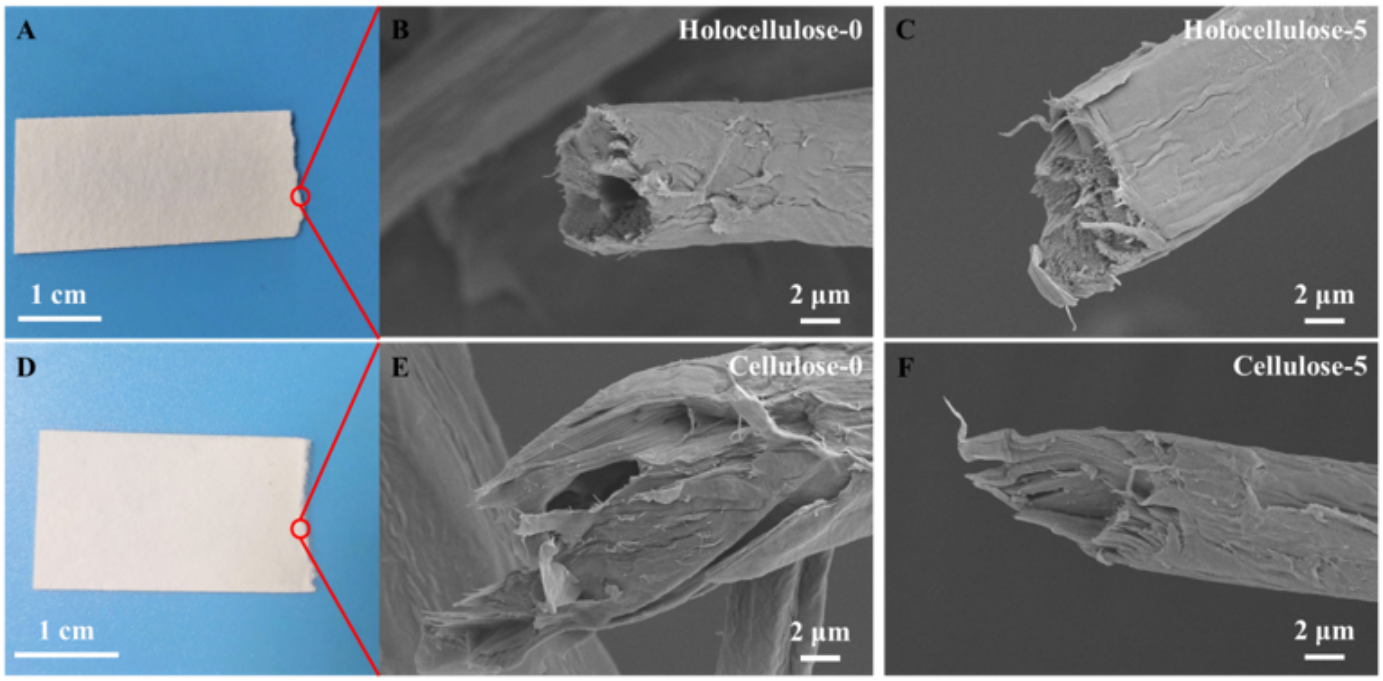

Figure 4

Fracture surfaces of papers: (A) holocellulose-0 and (D) celloluse-0. SEM image of the fiber structure at the paper break: the fiber of (B) holocellulose-0, (C) holocellulose-0, (E) cellulose-0 and (F) cellulose-5.

Supplementary Files

This is a list of supplementary files associated with this preprint. Click to download.

- Cellulosesupportinginformation.docx
- TableofContent.docx